Front. Optoelectron. 2014, 7(1): 74–76
DOI 10.1007/s12200-013-0374-2

RESEARCH ARTICLE

Multiband infrared luminescence of Er^{3+}-Ho^{3+}-Nd^{3+}/Tm^{3+}-codoped telluride glasses

Yaojing ZHANG[1], Lu SUN[1], Ying CHANG[2], Wenbin LI[3], Chun JIANG (✉)[1]

1 State Key Laboratory of Advanced Optical Communication Systems & Networks, Shanghai Jiao Tong University, Shanghai 200240, China
2 Digestive Endoscopic Center, Shanghai Sixth Hospital, Shanghai Jiao Tong University, Shanghai 200233, China
3 Medical Imaging Institute, Institute of Diagnostic and Interventional Radiology, Shanghai Sixth Hospital, Shanghai Jiao Tong University, Shanghai 200233, China

Abstract This paper reports the simultaneous emissions around 1.53, 1.80, 2.10, 2.70 and 3.00 μm in Er^{3+}-Ho^{3+}-Nd^{3+}/Tm^{3+}-codoped telluride glasses upon excitation of a conventional 808 nm laser diode. Both emission bands of 1.53 and 2.70 μm were assigned to the transitions of $^4I_{13/2}$ -$^4I_{15/2}$, $^4I_{11/2}$ -$^4I_{13/2}$ of Er^{3+} ions, respectively, the emission near 1.80 μm was assigned to the transition $^4F_4$ -$^4H_6$ of Tm^{3+} ions, and the emissions at 2.10 and 3.00 μm arose from the transitions of $^5I_7$ -$^5I_8$, $^5I_6$ -$^5I_7$ of Ho^{3+} ions. The materials are promising for ultra-broad band amplified spontaneous emission optical sources at near and middle infrared region.

Keywords multiband luminescence, Er^{3+}-Ho^{3+}-Nd^{3+}/Tm^{3+}, telluride glass

1 Introduction

Presently, near- and mid-infrared lasers operating in the wavelength region around 1.5–3.0 μm are attracting interest of researcher in fields of optical communication, medical surgery, eye-safe laser radar, remote sensing, atmosphere pollution monitoring, and so on. New materials, which are used to produce these lasers, are being searched. The glass, crystal and rare-earth ions should be considered because the hosts for dopants are cost-effective and easy to produce in large scale, and rare-earth materials are abundant in natural source. Rare-earth doped fluoride, fluoro-phosphate glasses [1–3], telluride and fluoro-telluride glasses [4–11], chalcohalide glasses [12,13] and other hosts [14–18] as well as fiber devices [19–23] for mid-infrared luminescence have been reported, and nearly all the literatures concentrated on the single emission at 2.70 μm or other wavelengths.

Received August 14, 2013; accepted October 9, 2013

E-mail: cjiang@sjtu.edu.cn

In our present work, we simultaneously observe the multiband emissions around 1.53, 2.10, 2.70 and 3.00 μm in Er^{3+}-Ho^{3+}-Nd^{3+}-codoped telluride glasses, and the multiband emissions around 1.53, 1.80, 3.00 μm in Er^{3+}-Ho^{3+}-Tm^{3+}-codoped telluride glasses with the excitation of 808 nm pump laser diode.

2 Fabrication and experiment

The Er^{3+}-Ho^{3+}-Nd^{3+}-codoped system has the following compositions (in mol %): $70TeO_2$-$20ZnO$-$9.0CaO$-$0.6Er_2O_3$-$0.1Ho_2O_3$-$0.3Nd_2O_3$ (EHN), and the Er^{3+}-Ho^{3+}-Tm^{3+}-codoped system (EHT) has the same compositions as EHN, but Nd_2O_3 is replaced by Tm_2O_3.

The samples were prepared with conventional melting method. Before melting powders in a Si-C electric resistance furnace, the compositions were weighted and mixed. The mixtures were melted and homogenized at 800°C–900°C in an Al_2O_3 crucible in the furnace. The melting was poured onto a preheated brass mold and annealed for 3 hours around 100°C in a muffle furnace, and then cooled inside the furnace by turning the power supply off. The samples were cut and polished to form a plate shape with the size 10 mm × 10 mm × 1 mm for emission spectra measurements.

The near- and mid-infrared (mid-IR) emission spectra of the samples were measured with excitation of an 808 nm laser diode at room temperature by a Traix 320 type spectrometer (Jobin-Yvon Co., France) with resolution of 1 nm and detectable wavelength range 1.0–3.0 μm.

3 Results and discussion

The near- and mid-IR photoluminescence spectrum of the EHN is shown in Fig. 1. As can be seen, its peaks are at 1.53, 2.10, 2.70 and 3.00 μm, which correspond to the

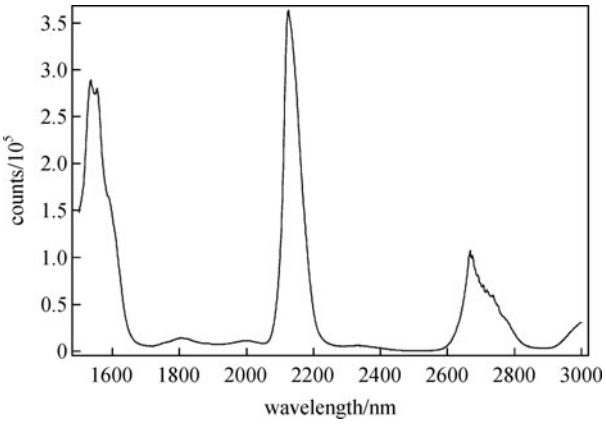

Fig. 1 Multiband emissions around 1.53, 2.10, 2.70 and 3.00 μm in Er^{3+}-Ho^{3+}-Nd^{3+}-codoped (EHN) telluride glasses upon excitation of a conventional 808 nm laser diode

transitions Er^{3+}: $^4I_{13/2} \rightarrow {}^4I_{15/2}$, Ho^{3+}: $^5I_7 \rightarrow {}^5I_8$, Er^{3+}: $^4I_{11/2} \rightarrow {}^4I_{13/2}$ and Ho^{3+}: $^5I_6 \rightarrow {}^5I_7$, respectively. The photoluminescence spectrum of the EHT is shown in Fig. 2, its peaks are at 1.53, 1.80, 3.00 μm, which correspond to the transitions Er^{3+}: $^4I_{13/2} \rightarrow {}^4I_{15/2}$, Tm^{3+}: $^4F_4$ -$^4H_6$ and Ho^{3+}: $^5I_6 \rightarrow {}^5I_7$, respectively.

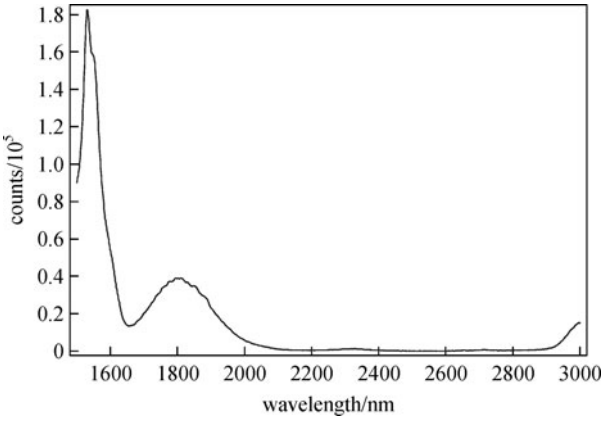

Fig. 2 Multiband emissions around 1.53,1.80, 3.00 μm in Er^{3+}-Ho^{3+}-Tm^{3+}-codoped (EHT) telluride glasses upon excitation of a conventional 808 nm laser diode

The processes of electron transitions and energy transfers in EHN and EHT systems are schematically shown in Figs. 3 and 4.

In EHN system, under the excitation of 808 nm laser diode, the electrons at the ground states $^4I_{9/2}$ of Nd^{3+}, $^4I_{15/2}$ of Er^{3+} and $^5I_8$ of Ho^{3+} are excited to the states $^4F_{3/2}$ of Nd^{3+} and $^4I_{9/2}$ of Er^{3+} and $^5I_5$ of Ho^{3+}, respectively. Due to smaller energy level difference between $^4F_{3/2}$ of Nd^{3+} and $^4I_{9/2}$ of Er^{3+}, $^4F_{3/2}$ of Nd^{3+} and $^5I_5$ of Ho^{3+}, the energy at the excited state ($^4F_{3/2}$) of Nd^{3+} is transferred (ET1,ET2) to $^4I_{9/2}$ of Er^{3+} and $^5I_5$ of Ho^{3+}. For Er^{3+} ions, the electrons at the excited state relax into $^4I_{11/2}$, then further transit into

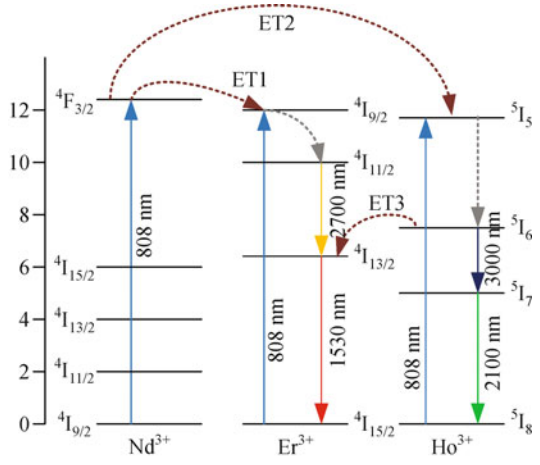

Fig. 3 Processes of electronic transitions and energy transfers in $70TeO_2$-20ZnO-9.0CaO-$0.6Er_2O_3$-$0.1Ho_2O_3$-$0.3Nd_2O_3$ systems (EHN) upon excitation of a conventional 808 nm laser diode

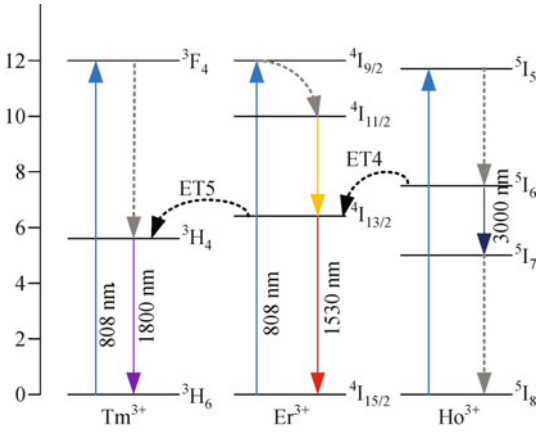

Fig. 4 Processes of electronic transitions and energy transfers in $70TeO_2$-20ZnO-9.0CaO-0.6 Er_2O_3-$0.1Ho_2O_3$-$0.3Tm_2O_3$ systems (EHT) upon excitation of a conventional 808 nm laser diode

$^4I_{13/2}$, $^4I_{15/2}$, with the emissions around 2.70, 1.53 μm. For Ho^{3+} ions, the electrons at the excited state relax into $^5I_6$, then further transit into $^5I_7$, $^5I_8$, with the emissions around 3.00, 2.10 μm.

In EHT system, under the same excitation as the system above, the electrons at the ground states $^3H_6$ of Tm^{3+}, $^4I_{15/2}$ of Er^{3+} and $^5I_8$ of Ho^{3+} are excited to the states $^3F_4$ of Tm^{3+} and $^4I_{9/2}$ of Er^{3+} and $^5I_5$ of Ho^{3+}. Due to smaller energy level difference between $^5I_6$ of Ho^{3+} and $^4I_{13/2}$ of Er^{3+}, $^4I_{13/2}$ of Er^{3+} and $^3H_4$ of Tm^{3+}, a fraction of energy at $^5I_5$ of Ho^{3+} is transferred (ET3) to $^4I_{13/2}$ of Er^{3+}, and a fraction of energy at $^4I_{13/2}$ of Er^{3+} is transferred (ET4) to $^3H_4$ of Tm^{3+}. For Tm^{3+} ions, meanwhile, the electrons at the excited state relax into $^3H_4$, then further transit into the ground state $^4H_6$, with emissions around 1.80 μm. For Ho^{3+} ions, the electrons at the excited state relax into $^5I_6$, then further transit into $^5I_7$ with emissions around 3.00 μm. For Er^{3+}

ions, the electrons at the excited state relax into $^4I_{11/2}$, $^4I_{13/2}$, then transit into $^4I_{15/2}$, with emissions around 1.53 μm.

Additionally, it is shown in Figs. 1 and 2 that the emission bands at 2.10 and 2.70 μm in EHN system disappear in EHT system. It can be explained that in the latter, due to smaller energy level difference between $^5I_6$ of Ho^{3+} and $^4I_{13/2}$ of Er^{3+}, $^4I_{13/2}$ of Er^{3+} and $^3H_4$ of Tm^{3+}, a fraction of energy at $^5I_6$ of Ho^{3+} is transferred into the $^4I_{13/2}$ of Er^{3+}, and a fraction of whose energy is transferred into $^3H_4$ of Tm^{3+}. Consequently, the electron population inversions between the $^5I_7$ and $^5I_8$ of Ho^{3+} and between the $^4I_{11/2}$ and $^4I_{13/2}$ of Er^{3+} are so weak that the emissions caused by the transitions are too weak to be detected.

4 Conclusions

In conclusion, we presented Er^{3+}-Ho^{3+}-Nd^{3+}- and Er^{3+}-Ho^{3+}-Tm^{3+}-codoped telluride glasses. With excitation of a conventional 808 nm laser diode, the multiband emissions around 1.53, 1.80, 2.10, 2.70 and 3.00 μm were observed. The emission bands 1.53 and 2.70 μm were assigned to the transitions of $^4I_{13/2}$-$^4I_{15/2}$, $^4I_{11/2}$ -$^4I_{13/2}$ of Er^{3+} ions, respectively, and 1.80 μm was assigned to the transition $^4F_4$ -$^4H_6$ of Tm^{3+} ions, and the emissions at 2.10 and 3.00 μm arose from the transitions of $^5I_7$ -$^5I_8$, $^5I_6$ -$^5I_7$ of Ho^{3+} ions. The materials will be potential in use of ultra broad band amplified spontaneous emission optical sources at near- and mid-IR region.

References

1. Tian Y, Xu R R, Zhang L Y, Hu L L, Zhang J J. Observation of 2.7 μm emission from diode-pumped Er^{3+}/Pr^{3+}-codoped fluorophosphate glass. Optics Letters, 2011, 36(2): 109–111
2. Xu R R, Tian Y, Hu L L, Zhang J J. Enhanced emission of 2.7 μm pumped by laser diode from Er^{3+}/Pr^{3+}-codoped germanate glasses. Optics Letters, 2011, 36(7): 1173–1175
3. Tian Y, Xu R R, Hu L L, Zhang J J. Intense 2.7 μm and broadband 2.0 μm emission from diode-pumped Er^{3+}/Tm^{3+}/Ho^{3+}-doped fluorophosphate glass. Optics Letters, 2011, 36(16): 3218–3220
4. Fan J, Yuan X, Li R, Dong H, Wang J, Zhang L. Intense photoluminescence at 2.7 μm in transparent Er^{3+}: CaF_2-fluorophosphate glass microcomposite. Optics Letters, 2011, 36(22): 4347–4349
5. Sandrock T, Diening A, Huber G. Laser emission of erbium-doped fluoride bulk glasses in the spectral range from 2.7 to 2.8 μm. Optics Letters, 1999, 24(6): 382–384
6. Zhong H Y, Chen B J, Ren G Z, Cheng L H, Yao L, Sun J S. 2.7 μm emission of Nd^{3+}, Er^{3+}codoped tellurite glass. Journal of Applied Physics, 2009, 106(8): 083114-1–083114-3
7. Guo Y Y, Li M, Tian Y, Xu R R, Hu L L, Zhang J J. Enhanced 2.7 μm emission and energy transfer mechanism of Nd^{3+}/Er^{3+} codoped sodium tellurite glasses. Journal of Applied Physics, 2011, 110(1): 013512-1–013512-5
8. Tsang Y, Richards B, Binks D, Lousteau J, Jha A. A Yb^{3+}/Tm^{3+}/Ho^{3+} triply-doped tellurite fibre laser. Optics Express, 2008, 16(14): 10690–10695
9. Zhou B, Tao L, Tsang Y H, Jin W, Pun E Y B. Superbroadband near-IR photoluminescence from Pr^{3+}-doped fluorotellurite glasses. Optics Express, 2012, 20(4): 3803–3813
10. Zhou B, Tao L, Tsang Y H, Jin W, Pun E Y B. Superbroadband near-infrared emission and energy transfer in Pr^{3+}-Er^{3+} codoped fluorotellurite glasses. Optics Express, 2012, 20(11): 12205–12211
11. Zhou B, Tao L, Jin W, Tsang Y H, Pun E Y B. Superbroadband NIR photoluminescence in Nd^{3+}/Tm^{3+}/Er^{3+} codoped fluorotellurite glasses. IEEE Photonics Technology Letters, 2012, 24(11): 924–926
12. Xu Y, Chen D, Wang W, Zhang Q, Zeng H, Shen C, Chen G. Broadband near-infrared emission in Er^{3+}-Tm^{3+} codoped chalcohalide glasses. Optics Letters, 2008, 33(20): 2293–2295
13. Lin H, Chen D, Yu Y, Yang A, Wang Y. Enhanced mid-infrared emissions of Er^{3+} at 2.7 μm via Nd^{3+} sensitization in chalcohalide glass. Optics Letters, 2011, 36(10): 1815–1817
14. Zhou B, Lin H, Chen B, Pun E Y B. Superbroadband near-infrared emission in Tm-Bi codoped sodium-germanium-gallate glasses. Optics Express, 2011, 19(7): 6514–6523
15. Zhang Q, Ding J, Shen Y, Zhang G, Lin G, Qiu J, Chen D. Infrared emission properties and energy transfer between Tm^{3+} and Ho^{3+} in lanthanum aluminum germanate glasses. Journal of the Optical Society of America. B, 2010, 27(5): 975–980
16. Liu X, Qiao Y, Dong G, Ye S, Zhu B, Lakshminarayana G, Chen D, Qiu J. Cooperative downconversion in Yb^{3+}/-RE^{3+} (RE = Tm or Pr) codoped lanthanum borogermanate glasses. Optics Letters, 2008, 33(23): 2858–2860
17. Zhang W J, Zhang Q Y, Chen Q J, Qian Q, Yang Z M, Qiu J R, Huang P, Wang Y S. Enhanced 2.0 μm emission and gain coefficient of transparent glass ceramic containing BaF_2: Ho^{3+}, Tm^{3+} nanocrystals. Optics Express, 2009, 17(23): 20952–20958
18. Chen D, Wang Y, Yu Y, Liu F, Huang P. Sensitized thulium ultraviolet upconversion luminescence in Tm^{3+}/Yb^{3+}/Nd^{3+} triply doped nanoglass ceramics. Optics Letters, 2007, 32(21): 3068–3070
19. Zhu X, Jain R. Numerical analysis and experimental results of high-power Er/Pr:ZBLAN 2.7 μm fiber lasers with different pumping designs. Applied Optics, 2006, 45(27): 7118–7125
20. Neely T W, Johnson T A, Diddams S A. High-power broadband laser source tunable from 3.0 μm to 4.4 μm based on a femtosecond Yb:fiber oscillator. Optics Letters, 2011, 36(20): 4020–4022
21. Pollnau M, Ghisler C, Lüthy W, Weber H P, Schneider J, Unrau U B. Three-transition cascade erbium laser at 1.7, 2.7, and 1.6 μm. Optics Letters, 1997, 22(9): 612–614
22. Park Y H, Lee D W, Kong H J, Kim Y S. Dynamics of a flashlamp pumped 2.70 μm emission Cr:Er:YSGG laser with an infrared-quartz FTIR shutter. Journal of the Optical Society of America. B, 2008, 25(12): 2123–2129
23. Zhu Z, Li J, You Z, Wang Y, Lv S, Ma E, Xu J, Wang H, Tu C. Benefit of Pr^{3+} ions to the spectral properties of Pr^{3+}/Er^{3+}: $CaGdAlO_4$ crystal for a 2.7 μm laser. Optics Letters, 2012, 37(23): 4838–4840